



# HHS Public Access

Author manuscript

*J Sound Vib.* Author manuscript; available in PMC 2015 December 07.

Published in final edited form as:

*J Sound Vib.* 2013 November 25; 332(24): 6193–6202. doi:10.1016/j.jsv.2013.07.017.

## Theoretical relationship between vibration transmissibility and driving-point response functions of the human body

Ren G. Dong\*, Daniel E. Welcome, Thomas W. McDowell, and John Z. Wu

Engineering & Control Technology Branch, National Institute for Occupational Safety and Health, Morgantown, WV 26505, USA

### Abstract

The relationship between the vibration transmissibility and driving-point response functions (DPRFs) of the human body is important for understanding vibration exposures of the system and for developing valid models. This study identified their theoretical relationship and demonstrated that the sum of the DPRFs can be expressed as a linear combination of the transmissibility functions of the individual mass elements distributed throughout the system. The relationship is verified using several human vibration models. This study also clarified the requirements for reliably quantifying transmissibility values used as references for calibrating the system models. As an example application, this study used the developed theory to perform a preliminary analysis of the method for calibrating models using both vibration transmissibility and DPRFs. The results of the analysis show that the combined method can theoretically result in a unique and valid solution of the model parameters, at least for linear systems. However, the validation of the method itself does not guarantee the validation of the calibrated model, because the validation of the calibration also depends on the model structure and the reliability and appropriate representation of the reference functions. The basic theory developed in this study is also applicable to the vibration analyses of other structures.

### 1. Introduction

Prolonged, intensive exposure to human vibration may cause various injuries and disorders [1]. The biodynamic responses of the human body to vibration such as vibration stresses, strains, and power absorption density are likely to play an important role of the mechanisms of such injuries and disorders [2]. Therefore, the study of these responses can improve the understanding of their mechanisms and help in quantifying vibration exposures for risk assessments. Furthermore, knowledge of the biodynamic responses is also important for the design and analysis of vehicle seats, powered hand tools, and vibration-reducing devices and their test apparatuses.

\* Correspondence to: ECTB/HELD/NIOSH/CDC, 1095 Willowdale Road, MS L-2027, Morgantown, WV 26505, USA. Tel.: +1 304 285 6332; fax: +1 304 285 6265. rkd6@cdc.gov (R.G. Dong)..

#### Disclaimers

The content of this publication does not necessarily reflect the views or policies of the National Institute for Occupational Safety and Health (NIOSH), nor does mention of trade names, commercial products, or organizations imply endorsement by the U.S. Government.

Probably because no in-vivo method has been developed to reliably measure the biodynamic responses inside the human body, and the overall biodynamic responses of the system are of primary concern in the designs and analyses of mechanical equipment or devices, the biodynamic responses have been most frequently studied by examining the directly-measurable vibration transmissibility along with the driving-point response function (DPRF) most frequently expressed as apparent mass and mechanical impedance of the human whole body or a segment. These two types of frequency response functions are measured at different locations on the body, and they reflect some different aspects of the overall dynamic properties of the system. Hence, it is generally hypothesized that the combined knowledge of these two types of response functions and their relationship may not only enhance the understanding of the biodynamic responses, but such understanding can also help the development of more reliable biodynamic models of the system for the above-mentioned applications [3–5].

Several studies have investigated the relationship using measured vibration transmissibility and apparent mass or mechanical impedance of the human whole body or hand-arm system [3,5–8]. While some correlations in their resonance characteristics in some vibration directions were observed, none of these studies identified their exact relationships. Observing that the apparent mass of a one degree-of-freedom (1-DOF) model can be expressed explicitly as a function of its mass and transmissibility [9], we generally hypothesize that a similar relationship between these two types of response functions exists in other vibration systems or models. The objective of this study is to identify the exact form of this relationship. Different from previous studies, this study uses a classic theoretical approach to derive the relationship. The identified relationship is also verified using several models of the human whole body and hand-arm system. As an example application, the developed theory is also used to perform a preliminary analysis of a popular method for determining or calibrating the parameters of human vibration models.

## 2. Derivation of the theoretical relationship between vibration transmissibility and driving-point response functions

To help derive the relationship, a general conceptual model of the human body is proposed and shown in Fig. 1. This figure does not represent any specific model of the human body, but it shows some possible boundary conditions, interactions, and responses associated with the vibration exposure. While the vibration exposure can exist in all the three translational directions ( $x$ ,  $y$ ,  $z$ ) and three rotational orientations ( $r_x$ ,  $r_y$ ,  $r_z$ ), only the accelerations and dynamic force responses in the  $z$  direction are represented in the figure. These are used to describe the basic process for deriving the relationship theory established in this study. The vibration transmissibility or motion transfer function ( $T_z$ ) at a point on the body in the  $z$  direction is conventionally defined as follows:

$$T_z = \ddot{Z} / \ddot{Z}_0 \quad (1)$$

where  $\ddot{Z}$  is the vibration acceleration at the point of interest, and  $\ddot{Z}_0$  is the excitation acceleration input to the system. The transmissibility is a complex function, which can be expressed as magnitude and phase angle in the frequency domain. The vibration input in one

direction can also generate responses in the other directions [10,11]. If the motion response in any other direction is used to evaluate the motion transfer function, the function is termed as cross-axis transmissibility.

The driving-point response function is also a complex function, and it is conventionally defined as the ratio of the dynamic force ( $F_Z$ ) and motion measured at the driving point [1,9]. Depending on the input motion metric (displacement –  $Z_0$ , velocity –  $\dot{Z}_0$ , and acceleration –  $\ddot{Z}_0$ ) and the selection of the numerator and denominator in the ratio, the DPRF can be expressed in several different forms such as apparent mass, mechanical impedance, dynamic stiffness, and compliance [1,9]. However, these expressions are not independent, and they can be transformed from one another in the frequency domain because the motion metrics can be derived from each other using the following formulas [1,9]:

$$\ddot{Z}_0 = j\omega \dot{Z}_0 = -\omega^2 Z_0 \quad \text{and} \quad j = \sqrt{-1} \quad (2)$$

To reduce the length of the descriptions, the apparent mass is used to represent the DPRF in the following presentations. For the z direction, the apparent mass ( $M_Z$ ) is expressed as follows:

$$M_Z = F_Z / \ddot{Z}_0 \quad (3)$$

If the dynamic force is that at the location of the excitation or input vibration, the response function evaluated from Eq. (3) is termed driving-point apparent mass. If the force is that from any other location of the system or its boundary, the function is termed cross-point apparent mass. If the force is in any direction other than the excitation direction, the function is termed cross-axis apparent mass.

According to Newton's second law, the sum of the dynamic forces acting at the driving points ( $\sum F_{Z_d}$ ) and those acting at the boundaries ( $\sum F_{Z_b}$ ) of the system shown in Fig. 1 is equal to the sum of the inertial forces distributed in the system ( $\int \ddot{Z} dm$ ) or

$$\sum F_{Z_d} + \sum F_{Z_b} = \int \ddot{Z} dm \quad (4)$$

Dividing Eq. (4) by input acceleration ( $\ddot{Z}_0$ ) and applying Eqs. (1) and (3), the resulting relationship between apparent mass and vibration transmissibility in the z direction is derived as follows:

$$\sum M_{Z_d} + \sum M_{Z_b-d} = \int T_Z dm, \quad (5)$$

where  $M_{Z_d}$  is the apparent mass at each driving point,  $M_{Z_b-d}$  is the cross-point apparent mass at each boundary, and  $T_Z$  is the transmissibility of the individual mass elements distributed throughout the system.

Similarly, the relationship equation for each of the other two orthogonal directions ( $x$  and  $y$ ) is derived and it has exactly the same form as Eq. (5). The relationship between the rotational transmissibility (angular acceleration on the body divided by input/excitation angular acceleration) and the apparent inertia (dynamic torque at the system interface divided by angular acceleration at the driving point) in each rotational degree of freedom is also derived. It also has the same form as that shown in Eq. (5), except that the translational variables and parameters are replaced with rotational ones. Furthermore, although Eq. (5) is derived from the conceptual model of the human body, it is generally applicable to any other system because the human body in Fig. 1 can be replaced with any other structure. Therefore, Eq. (5) represents a generally applicable theorem, which is stated as follows:

The sum of the driving-point apparent mass and cross-point apparent mass at the interfaces of any system can be expressed as a linear combination of the motion transfer functions of the individual mass elements distributed throughout the system; the combination coefficient of each motion transfer function is its corresponding mass value.

While many studies did not or will not measure the cross-point apparent mass, this theorem is not directly applicable to many models. Alternatively, each boundary force can be expressed as a function of the boundary condition and the interaction motion at the boundary. Because the boundary force in each direction primarily depends on the boundary contact stiffness ( $K_{Zb}$ ) and damping ( $C_{Zb}$ ) in that direction and their related vibration displacement ( $Z$ ) and velocity ( $\dot{Z}$ ), the boundary force can be generally expressed as follows:

$$\sum F_{Zb} = - \sum (K_{Zb}Z + C_{Zb} \dot{Z}) \quad (6)$$

$K_{Zb}$  and  $C_{Zb}$  can be constant or variable parameters. When a nonlinear boundary condition is considered, each of these parameters can be expressed as a function of their influencing factors such as vibration magnitude, applied hand force, applied backrest force, applied footrest force, body posture, etc. Then, Eq. (4) can be written as follows:

$$\sum F_{Zd} = \int \ddot{Z} dm + \sum (K_{Zb}Z + C_{Zb} \dot{Z}) \quad (7)$$

dividing Eq. (6) by input acceleration ( $\ddot{Z}_0$ ) and applying Eqs. (1)–(3), the resulting relationship between apparent mass and vibration transmissibility in the  $z$  direction is alternatively derived as follows:

$$M_{ZTtotal} = \sum M_{Zd} = \int T_Z dm + \sum T_{Zb} (C_{Zb}/j\omega - K_{Zb}/\omega^2), \quad (8)$$

where  $M_{ZTtotal}$  is the total driving-point apparent mass, and  $T_{Zb}$  is the transmissibility of the mass element connected to the boundary. The comparison of Eqs. (5) and (8) indicates that

$$\sum M_{Zv-d} = - \sum T_{Zb} (C_{Zb}/j\omega - K_{Zb}/\omega^2) \quad (9)$$

the two terms in the parenthesis of Eq. (9) can be termed as damping-induced equivalent mass and stiffness-induced equivalent mass, respectively. Then, the relationship theorem can be alternatively stated as follows:

The sum of the driving-point apparent mass of any system can be expressed as a linear combination of the motion transfer functions of the individual mass elements distributed throughout the system; the combination coefficient of each motion transfer function is the sum of its corresponding mass value and equivalent mass value related to boundary connecting stiffness and damping if applicable.

Eq. (8) is directly applicable to the vast majority of the human vibration models reported in the literature. For example, the relationship at each frequency ( $\omega$ ) for the hand-arm model shown in Fig. 2(d) is expressed as follows:

$$M_{\text{Hand}}(\omega) = M_{\text{Fingers}}(\omega) + M_{\text{Palm}}(\omega) = m_{01} + m_{02} + T_1(\omega) m_1 + T_2(\omega) m_2 + T_3(\omega) + \left[ m_3 + c_5/j\omega - k_5/\omega^2 \right] \quad (10)$$

where  $M_{\text{Hand}}$  is the apparent mass of the entire hand-arm system,  $M_{\text{Fingers}}$  is the apparent mass at the fingers, and  $M_{\text{Palm}}$  is the apparent mass at the palm. Similarly, the relationships for the other models shown in Fig. 2 were also written. They were used to verify Eq. (8). The normal parameter values used in this study are listed in Table 1, which were collected from the reported studies [4,12,13]. The modeling results confirm the derived theorem.

It is emphasized that the theorem is directly derived from the well-established classic principle without applying any artificial constraints or the technical treatments of the variables, and parameters of the system and the mathematical operations used in the derivation do not involve in any linear assumption. Therefore, the theorem is valid for both linear and nonlinear systems.

The theorem is also applicable for representing the relationship between the cross-axis apparent mass and the cross-axis transmissibility in each non-excitation direction, except that the stiffness and damping values for that direction are required in the equation. In cases of multi-axis excitations, each type of response in a given direction is generally the combination of the principal and cross-axis responses. Eq. (8) is also applicable to the relationship in each direction, providing that the response functions are calculated with respect to the input vibration in the same direction. This is because the multi-axis excitations and responses do not affect the validity of Newton's second law, but the same reference excitation (e.g.,  $\ddot{z}_0$  in the  $z$  direction) is required to derive Eq. (5) from Eq. (4) or to derive Eq. (8) from Eq. (7).

The excitations at different locations/points of the interface in each direction may vary greatly. For example, the vibration at the footrest may be significantly different from that on the seat pan of a suspended chair. Eq. (8) cannot be directly used for such a case because it requires the same input vibration in each direction. However, the combination of Eq. (5) and Eq. (8) can be used to write an equation for each of the excitations of a system. For example, if the footrest vibration is different from the seat vibration shown in Fig. 1, the relationship equations for the excitations separately applied at the footrest and seat can be written as follows:

$$M_{Z_{\text{Foot}-F}} + M_{Z_{\text{Seat}-F}} = \int T_{Z-F} dm + \sum T_{Zb-F} (C_{Zb}/j\omega - K_{Zb}/\omega^2) \quad (11)$$

$$M_{Z_{\text{Foot}-S}} + M_{Z_{\text{Seat}-S}} = \int T_{Z-S} dm + \sum T_{Zb-S} (C_{Zb}/j\omega - K_{Zb}/\omega^2) \quad (12)$$

where ‘F’ is denoted the excitation at the footrest and ‘S’ is the excitation at the seat. These two equations can be combined to form the following equation:

$$M_{Z_{\text{Foot}-F}} + M_{Z_{\text{Seat}-F}} + M_{Z_{\text{Foot}-S}} + M_{Z_{\text{Seat}-S}} = \int (T_{Z-F} + T_{Z-S}) dm + \sum (T_{Zb-F} + T_{Zb-S}) (C_{Zb}/j\omega - K_{Zb}/\omega^2) \quad (13)$$

These equations may be useful for further studying the cross-point responses and the multi-point excitation responses.

### 3. Representative transmissibility function

The human body is a continuous biomechanical system, and its vibration transmissibility generally varies with location and direction [5,14]. For a finite element model with sufficient meshing, it may be acceptable to use the transmissibility directly measured at a point on a substructure to represent the transmissibility at the corresponding location in the model. However, this may not be acceptable for a lumped-parameter model. Each transmissibility function required in the above equations should be sufficiently representative of the overall vibration of the corresponding substructure simulated as a lumped mass in such a model. Similar to the derivation of Eq. (5) or (8), the equivalent or representative transmissibility ( $T_S$ ) of a substructure in each direction is derived as follows:

$$T_S = \frac{1}{m_S} \int T(x, y, z) dm = \frac{1}{m_S} \int T(x, y, z) \rho(x, y, z) dx dy dz, \quad (14)$$

where ‘S’ is referred to a substructure,  $m_S$  is its lumped mass of the substructure, and  $\rho$  is its mass density.

For example, the two mass elements ( $m_1$  and  $m_2$ ) in Model-c shown in Fig. 2 can be lumped together to form Model-b. While the lumped mass  $m_s = m_1 + m_2$ , its representative transmissibility is calculated from

$$T_S = \frac{1}{m_1 + m_2} (m_1 T_1 + m_2 T_2) \quad (15)$$

This example clearly demonstrates that the representative transmissibility is the average of the mass-weighted transfer functions distributed in a substructure simulated as a lumped mass in the model. Because the bones have larger mass densities than soft tissues, they have a larger weighting in the average. Unfortunately, it is difficult to measure the transmissibility on the bones inside the human body. It is also difficult to measure the transmissibility functions at a sufficient number of locations to synthesize accurately-representative transmissibility. Alternatively, the representative transmissibility may be estimated using a valid finite element model of each substructure, which remains a formidable research task.

## 4. An example of the theory application

The basic theory developed in this study can be used to enhance the understanding of the biodynamic responses and to help evaluate the modeling methods and develop better human vibration models. As an example, the theory was applied to perform a preliminary analysis of the calibration method that uses the combination of the transmissibility and DPRF to determine the parameters of the models [4,15–17].

### 4.1. A new approach for evaluating the calibration method

A critical assumption of the combined calibration method is that if the modeling response functions match the measured transmissibility and DPRF, the corresponding model parameters are unique and valid. Therefore, the evaluation of this study focused on tests of uniqueness and validity of the parameter solutions.

Practically, no experimental data can fully satisfy Eq. (5) or (8) for any model. This is primarily for the following reasons: (a) all experimental data include some measurement errors; (b) the transmissibility data measured on a human body do not fully meet the requirement of Eq. (14), or the measured transmissibility data do not perfectly represent the motion of a substructure simulated as a lumped mass in a model; and (c) any model is a certain approximation of the complex structure of the human body. Therefore, Eq. (5) or (8) cannot be directly used to reliably determine the model parameters with any experimental data. The calibration of a model is usually carried out by finding a set of model parameter values such that the modeling response functions can be fitted to the experimental data with the least root-mean-square error [4,15–17].

Also for the above-described reasons, it is technically difficult, expensive, and time-consuming to use the experimental approach to sufficiently test the uniqueness and validity of the combined calibration method. Furthermore, it is also difficult to clearly identify the error sources and to explore their solutions when any problems with the experimental data are confounded with those of the calibration method. To avoid experiment-induced uncertainties, an analytical method can be used to examine the calibration method. In the theoretical analyses, the response functions are assumed to be perfect for each model and to fully satisfy Eq. (5) or (8). This approach is practical only for some simple models such as a single degree of freedom model or the one shown in Fig. 2(a). It is very difficult to apply this approach to many other models, not only because their analytical response functions are very complex but also because the theoretical analyses require resolving very complex nonlinear equations. To avoid these difficulties and complexities, we proposed and applied an alternative approach to evaluate the calibration method in this study. Specifically, the values of the idealized or perfect response functions are calculated using the equations of motion of a model with specific parameters; these are used to represent the perfect response functions in the theoretical analyses using Eq. (5) or (8). This perfect function approach is equivalent to the analytical approach if the model parameter values have no impact on the overall outcome of the analyses. Hence, this approach actually takes advantage of the concept of the analytical approach and the simplicity of the numerical representations of the response functions while it avoids the problems of the experimental approach and the difficulties of the pure analytical approach.

Based on the above discussion, the major criteria for assessing the validation of a calibration method using the perfect function approach are proposed and summarized as follows: (i) the solution of the model parameters with the calibration method using the perfect response functions is unique, which addresses the uniqueness of the solution; (ii) the solutions of the model parameters are sufficiently converged with those used to calculate the perfect response functions, which addresses the validity of the solution; and (iii) the possible variations of the model parameters in the ranges of interest do not have any impact on the uniqueness or validation of the solution, which addresses the general applicability of the solution.

#### 4.2. General validation of the combined calibration method

Because the perfect response functions fully satisfy the relation equations, a group of linear algebraic equations for any model of interest can always be obtained from Eq. (5) or (8) by taking the function values at several frequencies. For example, a group of at least four equations for Model-c shown in Fig. 2 can be written as follows:

$$\begin{aligned} M_{\text{Total}}(6) &= m_0 + T_1(6) m_1 + T_2(6) m_2 + T_3(6) m_3 \\ M_{\text{Total}}(19) &= m_0 + T_1(19) m_1 + T_2(19) m_2 + T_3(19) m_3 \\ M_{\text{Total}}(48) &= m_0 + T_1(48) m_1 + T_2(48) m_2 + T_3(48) m_3 \\ M_{\text{Total}}(96) &= m_0 + T_1(96) m_1 + T_2(96) m_2 + T_3(96) m_3 \end{aligned} \quad (16)$$

If this group of equations is not singular, it can always be resolved to uniquely determine the mass values in the equations. The resulting mass values, together with the given transmissibility functions, can be used to determine a unique set of the remaining stiffness and damping parameters of the model [18]. These two-stage processes were tested using all the linear models shown in Fig. 2. Besides the model parameters listed in Table 1, randomly selected values of model parameters were also used in the tests. The resulting values of the model parameters are practically identical to their original values listed in Table 1. These analyses and tests indicate that the two-stage processes are generally applicable at least to any linear model. Therefore, the combined calibration method can generally meet all three criteria for its validation at least for linear models. Further studies are required to test its validation for nonlinear models.

#### 4.3. Potential problems and solutions of the combined calibration method

The above analyses indicate that the uniqueness and validity of the solution with the combined calibration method depends on the non-singularity of Eq. (16) for each model. This led to the identification of some potential problems of the calibration method. An obvious potential problem is that if any two transmissibility functions are identical, the corresponding Eq. (16) is singular; the solution cannot be unique. Identical transmissibility can theoretically occur if the model of the human body includes symmetrical branching substructures. This suggests that a certain constraint on the symmetry is required in the calibration of such a model.

While the vast majority of human vibration models do not include any symmetrical substructure, the measured transmissibility functions for calibrating the models may include



similar values within a certain frequency range. If such similar values constitute the major reference data used in a calibration, the problem for the numerical solution can be ill-defined; as a result, the parameters may be very sensitive to the perturbation of the experimental data or reference functions. To demonstrate this phenomenon, the transmissibility functions and the driving-point mechanical impedance of Model-c shown in Fig. 2 were calculated from the equations of motion of the model with the normal values of the parameters listed in Table 2, which are shown in Fig. 3. These perfect functions were used as references or target functions in the curve fitting process to determine the model parameters using the combined calibration method. While the comparisons of apparent mass functions are also shown in Fig. 3(b), the comparisons of the transmissibility functions are shown in Fig. 4. The curve fittings are almost perfect ( $r^2 = 1.000$ ). However, as indicated in Table 2, some of the resulting parameters are substantially different from the normal ones. This indicates that the solution of the model parameters is highly sensitive to the perturbations of the response functions. The high sensitivity is at least partially because the transmissibility functions on  $m_1$  and  $m_2$  are very similar at frequencies below 10 Hz, as shown in Fig. 3(a). In such a case, the theoretical validation of the combined calibration method may not guarantee a valid solution in the numerical calibrating process even if the perfect response functions are used as references in the calibration. This suggests that it is very important to check the solution sensitivity and to take some measures to reduce the sensitivity if necessary. It is hypothesized that the sensitivity may be reduced by decreasing the frequency weighting of the response functions in the low-frequency range where the large similarity occurs and/or by adding some tight constraints to the mass values in the numerical calibrating process. Further studies are required to test this hypothesis.

Moreover, the combined method may not be used to calibrate a model with multi-point driving points without providing all the driving-point response functions or applying some special constraints. For example, there are two driving points in Model-d shown in Fig. 2. Its corresponding Eq. (16) is singular because the two mass elements ( $m_{01}$  and  $m_{02}$ ) rigidly attached to the foundation of motion exhibit the same unity (1.0) transmissibility. As a result, it is impossible to determine the values of these two mass elements from the total apparent mass or mechanical impedance of the entire hand-arm system by directly applying the combined method. This problem can be resolved by utilizing the DPRFs distributed at both driving points (at the palm and fingers of the hand). This is because both mass elements are accounted for in the high-frequency response at each driving point. At a sufficiently high frequency, all the transmissibility values are close to zero; hence, each rigidly-attached mass can be estimated using its corresponding apparent mass at the high frequency or

$$M_{\text{Fingers}}(\text{high frequency}) \approx m_{01}, \quad M_{\text{Palm}}(\text{high frequency}) \approx m_{02} \quad (17)$$

Alternatively, a defined relationship between these two mass elements can be assumed to resolve the singular problem if only the total apparent mass or impedance is available for the model calibration, as used in the previous study [13].

It is also very important to note that the theoretical validity of the calibration method does not guarantee the validation of the calibrated model. This is because the validation of the

calibration also depends on the reliability of the measured response functions and the appropriate representation of the synthesized transmissibility functions used in the calibration. The driving-point response functions are generally more consistent and reliable than the transmissibility functions [5,19,20]. This suggests that less weighting should be given to the transmissibility than the DPRFs in the calibration. More importantly, because the transmissibility distributed on some substructures is spatial [14], according to Eq. (14), it is not reliable to use the transmissibility measured at a single point on the surface of each such substructure to sufficiently represent the overall vibration of the substructure. This further suggests that less relative weighting may be given to the transmissibility in the application of the combined method before a more reliable synthesis method is developed and used to create representative transmissibility functions for the model calibration. According to Eq. (5), the measurement and use of the cross-point response functions may also increase the reliability of the human vibration models. This may be a useful topic for further studies.

## 5. Conclusions

This study identified the basic theoretical relationship between vibration transmissibility and driving-point response functions of a linear or nonlinear system. Specifically, the sum of the driving-point response functions can be expressed as a linear combination of the transmissibility functions of the individual mass elements distributed throughout the system; the combination coefficients of each transmissibility function are its corresponding mass value and the equivalent mass values related to its boundary connecting stiffness and damping values if applicable. This study also clarified the requirements for reliably quantifying the transmissibility values used as references for calibrating system models. The example application of the developed theory demonstrated that the theory can be used to enhance the understanding of the biodynamic responses of the human whole body or segments, and it can serve as a theoretical basis for the further development and validation of human vibration models. This study also shows that theoretically, the combined method for the model calibration can result in a unique and valid solution, at least for linear systems. However, the validation of the method itself does not guarantee the validation of calibrated models; the developed theory also indicates that the validation of the model calibration depends not only on the calibration method but also on the model structure and the reliability and appropriate representation of the reference functions. Some potential sources of the problems with the combined calibration method are also identified and their potential solution methods are proposed. Although the basic theory presented in this paper is developed using the conceptual vibration model of the human body, it is generally applicable to the vibration analyses of other structures.

## References

- [1]. Griffin, MJ. Handbook of Human Vibration. Academic Press; London: 1990.
- [2]. Dong RG, Welcome DE, McDowell TW, Xu XS, Krajnak K, Wu JZ. A proposed theory on biodynamic frequency weighting for hand-transmitted vibration exposure. *Industrial Health*. 2012; 50(5):412–424. [PubMed: 23060254]

- [3]. Boileau P-É, Rakheja S, Yang X, Stiharu I. Comparison of biodynamic response characteristics of various human body models as applied to seated vehicle drivers. *Noise and Vibration Worldwide*. 1997; 28:7–14.
- [4]. Boileau P-É, Rakheja S, Wu X. A body mass dependent mechanical impedance model for applications in vibration seat testing. *Journal of Sound and Vibration*. 2002; 253(1):243–264.
- [5]. Wang W, Rakheja S, Boileau P-É. Relationship between measured apparent mass and seat-to-head transmissibility responses of seated occupants exposed to vertical vibration. *Journal of Sound and Vibration*. 2008; 314:907–922.
- [6]. Wu X, Rakheja S, Boileau P-É. Analyses of the relationships between biodynamic response function. *Journal of Sound and Vibration*. 1999; 226:595–606.
- [7]. Xu XS, Welcome DE, McDowell TW, Wu JZ, Wimer B, Warren C, Dong RG. The vibration transmissibility and driving-point biodynamic response of the hand exposed to vibration normal to the palm. *International Journal of Industrial Ergonomics*. 2011; 41(5):418–427.
- [8]. Zheng GT, Qiu Y, Griffin MJ. Vertical and dual-axis vibration of the seated human body: nonlinearity, cross-axis coupling, and associations between resonances in transmissibility and apparent mass. *Journal of Sound and Vibration*. 2012; 331(26):5880–5894.
- [9]. Harris, CM. *Shock and Vibration Handbook*. McGRAW-HILL; New York: 1995.
- [10]. Nawayseh N, Griffin MJ. Non-linear dual-axis biodynamic response to fore-and-aft whole-body vibration. *Journal of Sound and Vibration*. 2005; 282:831–862.
- [11]. Rakheja, S.; Dong, RG.; Welcome, DE.; Ahmed, AKW. The Proceedings of the 11th International Conference on Hand-Arm Vibration. Bologna, Italy: 2007. A preliminary study of cross-axis coupling effects in biodynamic response of the hand-arm system.
- [12]. Wei L, Griffin MJ. Mathematical models for the apparent mass of the seated human body exposed to vertical vibration. *Journal of Sound and Vibration*. 1998; 212(5):855–874.
- [13]. Dong RG, Rakheja S, McDowell TW, Welcome DE, Wu JZ. Estimation of the biodynamic responses distributed at fingers and palm based on the total response of the hand-arm system. *International Journal of Industrial Ergonomics*. 2010; 40(4):425–436.
- [14]. Welcome DE, Dong RG, Xu XS, Warren C, McDowell TW, Wu JZ. An investigation on the 3-D vibration transmissibility on the human hand-arm system using a 3-D scanning laser vibrometer. *Canadian Acoustics*. 2011; 39(2):44–45.
- [15]. Kim TH, Kim YT, Yoon YS. Development of a biomechanical model of the human body in a sitting posture with vibration transmissibility in the vertical direction. *International Journal of Industrial Ergonomics*. 2005; 35:817–829.
- [16]. Fritz M. An improved biomechanical model for simulating the strain of the hand-arm system under vibration stress. *Journal of Biomechanics*. 1991; 21:1165–1171. [PubMed: 1769981]
- [17]. Adewusi S, Rakheja S, Marcotte P. Biomechanical models of the human hand-arm to simulate distributed biodynamic responses for different postures. *International Journal of Industrial Ergonomics*. 2012; 42:249–260.
- [18]. Tregoubov VP. Problems of mechanical model identification for human body under vibration. *Mechanism and Machine Theory*. 2000; 35:491–504.
- [19]. Paddan GS, Griffin MJ. A review of the transmission of translational seat vibration to the head. *Journal of Sound and Vibration*. 1998; 215:863–882.
- [20]. Boileau P-É, Wu X, Rakheja S. Definition of a range of idealized values to characterize seated body biodynamic response under vertical vibration. *Journal of Sound and Vibration*. 1998; 215:841–862.

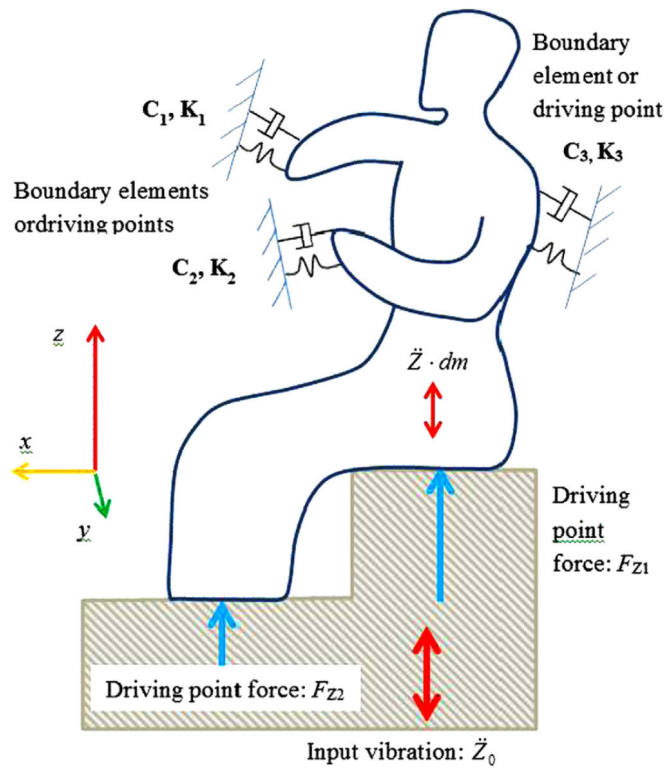


**Fig. 1.**  
A conceptual model of the human body vibration.

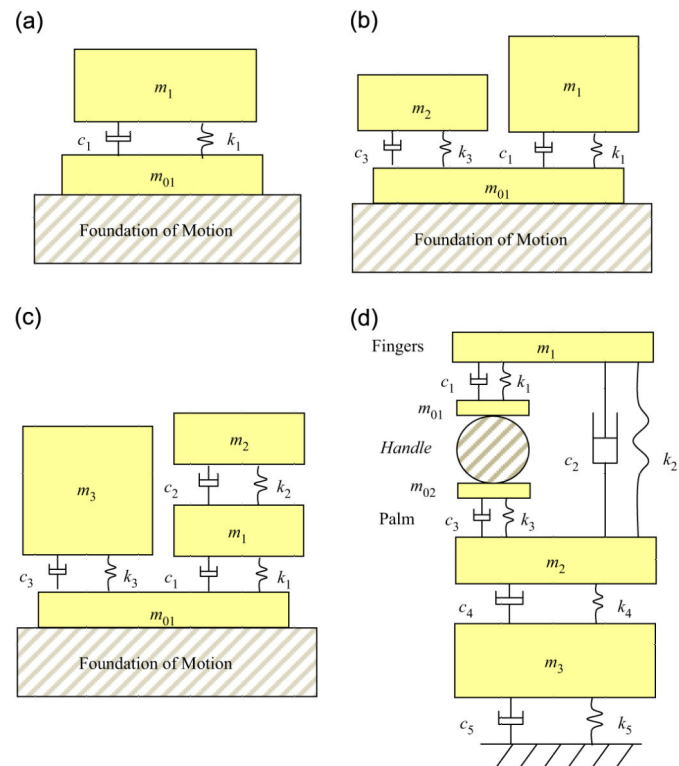


**Fig. 2.** Examples of whole-body and hand-arm models: (a) Model-a, a 2-DOF whole body [12]; (b) Model-b, a 3-DOF whole body model [12]; (c) Model-c, a 4-DOF whole body model [4]; and (d) Model-d, a five-DOF hand-arm system model [13].

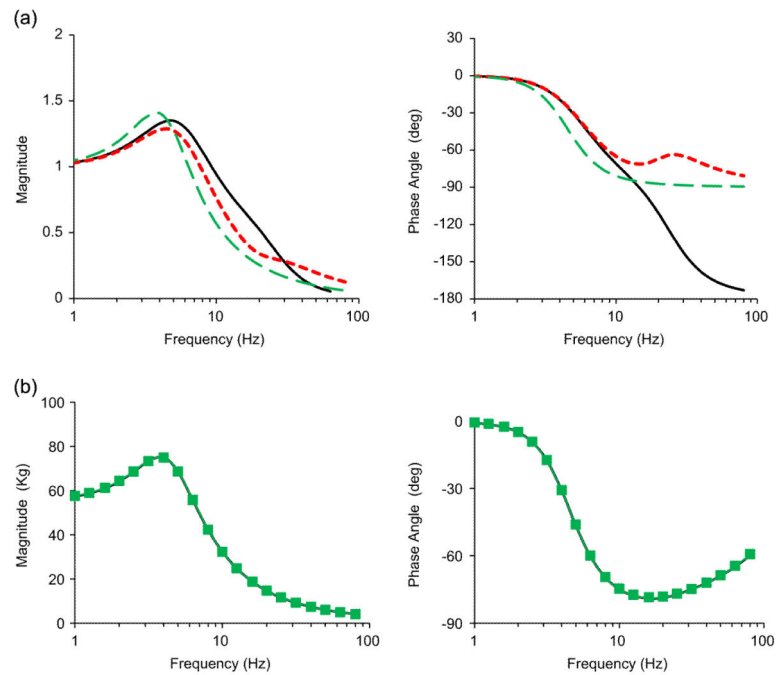


**Fig. 3.** Transmissibility and apparent mass functions of Model-c: (a) comparison of the transmissibility functions calculated using the normal parameters listed in Table 2 (— on  $m_1$ , — on  $m_2$ ; - - - on  $m_3$ ) and (b) comparison of the reference apparent mass calculated using the normal parameters listed in Table 2 and the matching apparent mass obtained from a numerical calibration using the references (— perfect reference; ■ matching apparent mass).

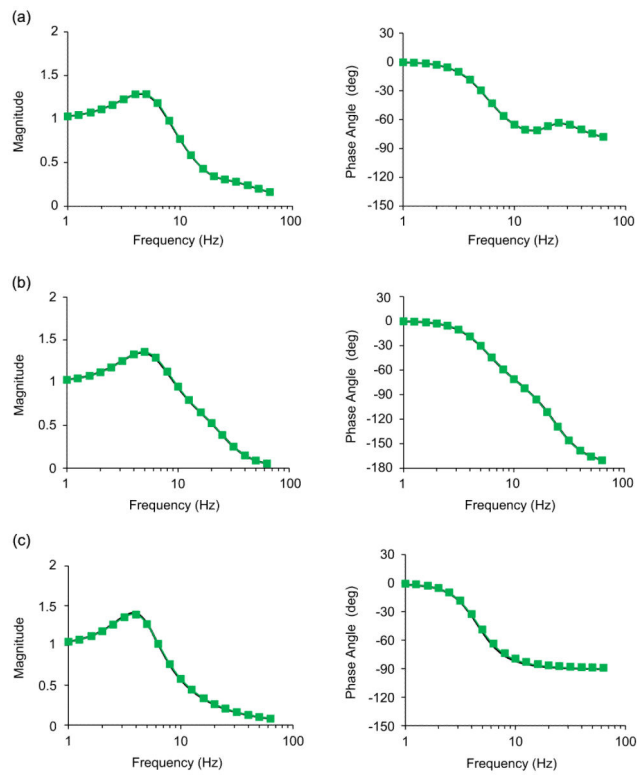


**Fig. 4.** Comparison of the reference transmissibility for Model-c and the matching transmissibility obtained from a numerical calibration (— perfect reference; ■ resulting function): (a) on  $m_1$ ; (b) on  $m_2$  and (c) on  $m_3$ .

**Table 1**

Parameter values of the models used in the mathematical tests of the proposed theory, which are collected from the reported studies [4,12,13].

Parameter	Unit	Model-a [12]	Model-b [12]	Model-c [4]	Model-d [13]
$m_{01}$	g	8600	7600	2000	10
$m_{02}$	g				20
$m_1$	g	50,200	37,400	6000	76
$m_2$	g		13,200	2000	1072
$m_3$	g			45,000	7500
$k_1$	N/m	51,987	39,071	10,000	176,880
$k_2$	N/m		42,867	34,400	12,000
$k_3$	N/m			36,200	44,220
$k_4$	N/m				18 91
$k_5$	N/m				8059
$c_1$	N s/m	1366	736	387	117
$c_2$	N s/m		609	234	40
$c_3$	N s/m			1390	84
$c_4$	N s/m				11 2
$c_5$	N s/m				93



**Table 2**

Comparisons of the normal parameter values from [4] and the calibration solutions of the parameters of Model-c using the combined method.

<b>Parameter</b>		<b>Normal or original value</b>	<b>Combined method</b>	
<b>ID</b>	<b>Unit</b>		<b>Parameter solution</b>	<b>Percent error (%)</b>
$m_0$	kg	2.00	2.02	1.03
$m_1$	kg	6.00	3.19	46.82
$m_2$	kg	2.00	1.10	44.93
$m_3$	kg	45.00	48.84	8.52
$k_1$	N/m	10,000.00	5532.11	84.73
$k_2$	N/m	34,400.00	18,837.27	41.51
$k_3$	N/m	36,200.00	39,760.19	8.75
$c_1$	N s/m	387.00	208.28	101.50
$c_2$	N s/m	234.00	127.30	147.65
$c_3$	N s/m	1390.00	1558.69	10.64

Author Manuscript

Author Manuscript

Author Manuscript

Author Manuscript